Effect of Fouling on the Performance of an Instream Turbine

Ralf Starzmann, Nicholas Kaufmann, Penny Jeffcoate,
Maricarmen Guerra, Alex Hay and Ray Pieroway

Abstract—**As the tidal energy industry starts to mature towards commercial projects a key focus is on reliable power performance. As for any marine application, fouling poses a potential performance reduction risk for instream turbine deployments.**

SCHOTTEL HYDRO have developed their current commercial SCHOTTEL Instream Turbines. Four drivetrains with 6.3m rotors were deployed on the surface platform PLAT-I by Sustainable Marine Energy. One of PLAT-Is key features is access to the turbines for inspection and maintenance in situ. The system has undergone sea testing from 2017 to 2021 in Scotland and Nova Scotia (Canada).

This paper presents the hydrodynamic rotor performance reduction due to fouling based on full-scale experimental results. An in-house blade element momentum model is used to quantify the changes of the hydrodynamic forces in terms of lift and drag for the hydrofoils used. Furthermore, the effect of fouling on the downstream wake was quanti-fied in the field. The performance reduction due to fouling is significant and leads to a power drop of up to 43%, whereas the thrust is reduced by 25%. This is also reflected in a reduction of the turbine's downstream wake as a "fouled" rotor extracts less energy from the flow. Modifica-tions of the polar data, used for semi-empirical performance predictions, are able to predict the effect of fouling on the rotor performance.

In general, the results derived from the testing prove the significance of access to the turbines in order to avoid reduc-tion in the turbines' performance due to fouling.

Keywords— **Full-Scale Testing, Performance, Fouling, SIT 250, Tidal Turbine.**

I. Introduction

Full-scale performance assessments of tidal instream turbines have been carried out for seabed mounted [1] as well as floating tidal turbines [2] [3]. Test guidelines and test methodologies are set out by the International Electrical Commission (IEC) in IEC62600-200, the technical specification for Tidal Energy Converter (TEC) power performance assessment [4].

Fouling poses a performance risk for instream turbine deployments, as for any long-term marine application where performance depends on boundary layer effects e.g. vessel drag). Any surface that is immersed in the sea undergoes a colonization process by which marine organisms can accumulate on the surface over time. Therefore, the hydrodynamic performance of an instream turbine blade, and hence its efficiency, is under the threat of marine fouling. The effect of fouling on the performance of instream turbines is hard to quantify.

So far only theoretical studies as well as model scale experiments have been published in the literature in order to show the effect of fouling on the performance of instream turbines. Mainly the relative surface roughness (k/c) has been used to quantify the fouling. The relative roughness is defined as the ratio of the roughness height k, to the chord length, c.

Investigations on the impact of fouling on a 1:5 scale cross-flow turbine with a model diameter of 172 mm showed that the impact of fouling on power output is substantial and, for the most severe cases, corresponding to $k/c = 0.035$, a 100% power reduction was found, while only a minimal reduction in thrust was measured [5]. Walker et al. investigated the effect of fouling on a 800mm horizontal axis turbine (at 1:25 scale), using model scale testing, as

Manuscript received 13 December, 2021; accepted 17 May, 2022; published 16 December, 2022.

This work been funded by the Federal Ministry for Economic Affairs and Energy of Germany (BMWi) in the project OsT (FKZ 03EE4001A) and by MITACS IT16896. Ralf Starzmann is with SCHOTTEL HYDRO, Mainzer Straße 99, 56321 Spay/Rhine, Germany (e-mail: rstarzmann@schottel.de).

Nicholas Kaufmann is with SCHOTTEL HYDRO Mainzer Straße 99, 56321 Spay/Rhine, Germany (e-mail: nkaufmann@schottel.de).

Penny Jeffcoate is with Sustainable Marine Energy, La Belle Esperance, The Shore, Edinburgh, UK (e-mail: penny.jeffcoate@sustainablemarine.com).

Maricarmen Guerra was with Dept. of Oceanography, Dalhousie University, Halifax, Nova Scotia, Canada, she is now with Universidad de Concepción; Chile (e-mail: marguerra@udec.cl)

Alex Hay is with Dept. of Oceanography, Dalhousie University, Halifax, Nova Scotia, Canada (e-mail: alex.hay@dal.ca)

Ray Pieroway is with Sustainable Marine Energy Canada, 95 Simmonds Drive, Dartmouth, Nova Scotia, B3B 1N7, Canada (e-mail: ray.pieroway@sustainablemarine.com).

Digital Object Identifier https://doi.org/10.36688/imej.5.229-237

well as predicting the turbines performance using a blade element momentum model (BEM) informed by wind tunnel experiments. The wind tunnel testing showed that both lift and drag coefficients are affected by fouling. A performance reduction of approx. 20% is reported for the rotor performance for both the BEM prediction and the experimental results. However the surface roughness for both cases was different, as $k/c = 0.002$ was used for the airfoil wind tunnel tests, whereas $k/c = 0.014$ was used for the model scale test of the rotor itself [6]. A detailed numerical study using computational fluid dynamics (CFD) was conducted by Song et al. to predict the fouling penalty of a 20m diameter horizontal axis instream turbine [7]. The surface roughness due to fouling was approximated by modifying the wall-function within the CFD model. Besides a decrease in power coefficient (~13%) a narrower optimum operating range, as well as a shift of the optimum tip speed ratio and a reduced thrust coefficient was found when analysing barnacle heights of 5mm, covering 20% of the blade surface.

This paper focuses on a field study, investigating the effect of fouling on the performance and downstream wake of instream turbines, with full scale field measurements carried out on Sustainable Marine Energy's multi-turbine platform PLAT-I 4.63, as deployed in Grand Passage (Nova Scotia, Canada). Furthermore a parametric study using an in-house BEM model is used to quantify the effect of increased drag on the respective hydrofoils.

The overall objectives of this work are:

- Compare the power and thrust performance of "clean" and "fouled" turbine rotors
- Evaluate the effect of the downstream wake for clean" and "fouled" turbine rotors
- Evaluate the effect of increased drag and reduced lift on the respective hydrofoils using an in-house BEM model
- Compare the predicted and measured turbine characteristics (power & thrust) for "clean" and "fouled" turbine rotors.

II. Inshore Floating Tidal Energy Platform

SCHOTTEL HYDRO together with Sustainable Marine Energy have developed their current SCHOTTEL Instream Turbines (SIT), on the surface floating inshore platform PLAT-I. The system has undergone sea testing using the 4m rotors between November 2017 and June 2018 in the UK and was deployed in Nova Scotia (Canada) from September 2018 to February 2021 with 6.3m rotors [8].

A. Overall Platform System

PLAT-I 4.63 is Sustainable Marine's first-generation floating platform, rated at 280 kW (i.e. four times 70 kW). Fig. 1 shows the platform in operation at Grand Passage, Nova Scotia. It is a three-hulled tidal energy platform that hosts four SIT 250 turbines. The platform self-aligns to incoming flow via a mooring turret, which is connected to a geostationary mooring spread. The turbines are suspended from the cross-deck, via lifting support structures called SIT Deployment Modules (SDMs). During normal operation, or when parked, the turbines are in the down configuration, but they can be lifted clear of the water for maintenance. The scheduled maintenance plan provides for a visual inspection of the turbines every six months, including but not limited to e.g. blades, housing, bolts and anodes. Fig. 2 shows the platform during blade installation in Grand Passage with two rotors in maintenance mode. So far no significant biofouling on the rotors has been found during testing, neither in Scotland nor in Canada. However during pre-longed times of non-operation rotors had been lifted clear of the water into the maintenance mode.

B. Instream Turbine

The SIT 250 is a horizontal axis instream turbine. The first generation SIT 250 was presented by SCHOTTEL in 2012. It is designed as a modular turbine system utilizing one drivetrain for two rotor diameters, 4m and 6.3m, which can be selected based upon the varying velocity frequency distributions of different deployment sites.

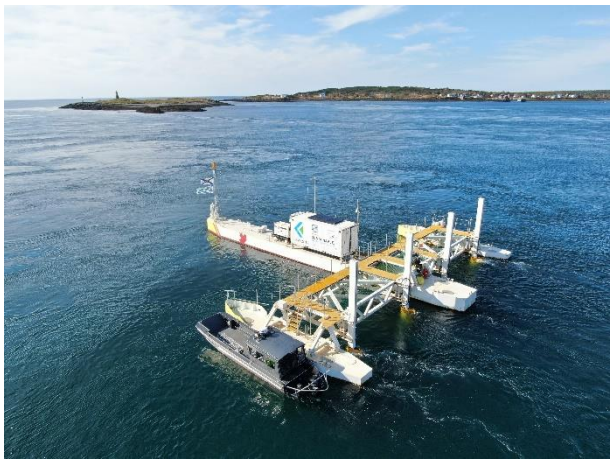

Fig. 1 PLAT-I 4.63 in operation as deployed in Grand Passage, Nova Scotia

Fig. 2 Blade installation (6.3m rotors) in Grand Passage

The larger rotor diameter is suited to lower flow speed sites, whereas the smaller rotor diameter is suited for

higher resource sites. The SIT 250 drive train is rated at the mechanical shaft, so rated power and grid-ready electrical power are P_{rated} = 85kW and P_{el} = 70kW respectively. Both three-bladed rotor versions are manufactured from composite material to provide passive-adaptive pitch behaviour. The blades are fitted onto a standardized hub with a diameter of 0.36 m. A rotor hub, slow speed shaft, planetary gearbox and asynchronous generator complete the drive train; the system is cooled by ambient water.

The full-scale turbine was extensively tested on Sustainable Marine's surface floating PLAT-I 4.40 platform (the same platform but using 4m rotors) and showed good agreement with semi-empirical power and thrust predictions using BEM [3]. On PLAT-I 4.63 the turbines operate in both clockwise and counter-clockwise direction (looking upstream), as shown in Fig. 3. The turbines are named SIT1 to SIT4 from Port to Starboard, Fig. 3. The hub deployment depth is 4.7m, whereas the horizontal spacing between the turbine hubs is 6.8m.

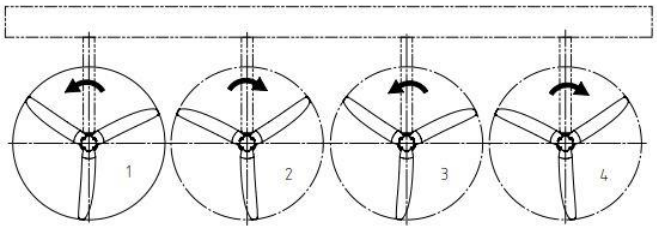

Fig. 3 Schematic SIT 250 configuration on PLAT-I

Table I summarizes the properties of the SIT 250 turbine system.

TABLE I
SIT 250 TURBINE SYSTEM

P_{rated}	rated power (mechanical)	85 kW
P_{el}	rated power (grid ready)	70 kW
-	pitch control	none (fixed-pitch)
-	variable speed control	yes
d_{hub}	hub diameter	0.36 m
d_{tip}	rotor diameter	6.3 m
d_{equ}	equivalent rotor diameter for PLAT-I turbine configuration according to [4]	12.3 m
h_{depth}	hub deployment depth	4.7 m
$h_{spacing}$	horizontal spacing between turbine hubs	6.8 m
λ_D	design tip speed ratio	6
$U_{0,rated}$	rated velocity	2.7 m/s
U_{cutout}	cut out velocity	5 m/s
$C_P(\lambda_D)$	power coefficient at the design point (rigid blade)	0.46
$C_T(\lambda_D)$	thrust coefficient at the design point (rigid blade)	0.75

III. EXPERIMENTAL SETUP

For the purpose of this study, full-scale field testing using the PLAT-I 4.63 platform was carried out at Grand Passage in Nova Scotia (Canada). All experimental results presented in this study are based on SIT 4, see Fig. 3. All experiments were carried out between October 13th and 19th 2020.

A. Test Site

The platform was deployed in Grand Passage at the southern tip of Digby Neck in September 2018. Digby Neck is a strip of land located at the mouth of the Bay of Fundy in Nova Scotia, Canada. Three channels – Grand Passage, Petit Passage and Digby Gut – cut through the Neck and have been deemed suitable for tidal power extraction [9]. Grand Passage is the westernmost of the three passages. It separates Brier Island to the west from Long Island to the east. The flood tide runs south to north through Grand Passage. In the middle of the channel there is only a small directional asymmetry in the flow and the current magnitudes on the flood and ebb tides are nearly symmetric [9]. Grand Passage provides for a very sheltered location with very moderate sea states, hence the effect of waves on the results reported hereafter is deemed to be negligible. A number of detailed site investigations including numerical and experimental work have been carried out to characterize the site conditions in Grand Passage [10][11][12].

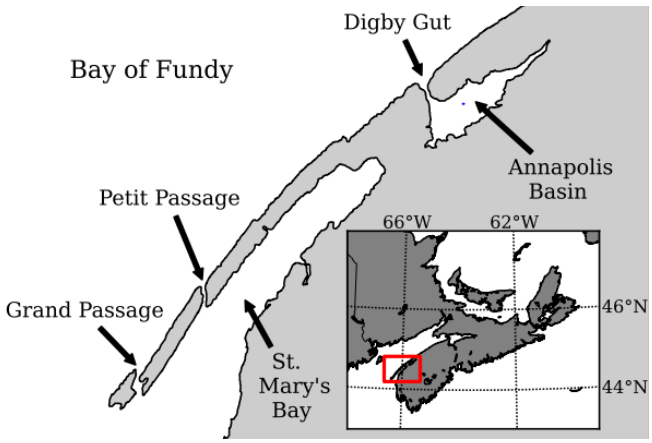

Fig. 4 Digby Neck region (Nova Scotia, Canada) [9]

B. Blade Conditions

All field testing carried out in this study was conducted for three blade conditions, being "clean", "fouled" and "cleaned PS". The "fouled" condition was achieved by keeping the rotor in the water without operating it for approx. four weeks. Fig. 5 shows the "clean" condition, whereas Fig. 6 shows the "fouled" configuration. The third condition "cleaned PS" was also tested, as the cleaning was carried out in two steps and as a first step only the pressure side (PS) was cleaned. Easy off-shore access to the turbine is one of PLAT-I's key features and cleaning of the rotors as carried out during this study is shown in Fig. 7.

An underlying biofilm was found on the "fouled" blades. Furthermore two dominant macro-fouling species of algae had been identified with a length of up to 10 cm. At 75% span of the blade the roughness height k was estimated to be between 2 mm - 10mm depending on the species as well as the density of the macro-fouling. This results in $k/c \approx 0.006$-0.03, providing a very wide range in terms of relative roughness. Therefore a realistic quantification of the non-dimensional roughness for the "fouled" rotor as investigated in this study is extremely difficult. Furthermore the characterization of drag solely based on k/c might be too simplistic, as the additional drag cause by fouling isn`t only effected by the roughness but also by the drag of the species themselves.

Fig. 5 SIT turbine rotors with "clean" blades

Fig. 6 SIT 4 rotor with "fouled" blades

Fig. 7 SIT 4 rotor during on site cleaning

C. Performance Testing

Instruments were mounted on the platform to measure the current velocity, turbine performance and reaction force at the SDM (due to rotor thrust and SDM drag). These are detailed in [8] and Fig. 8. The rotor thrust T was derived by resolving the forces acting on the SDM, including SDM drag, SDM and SIT masses, and rotor thrust, see [3] for more details.

The IEC standard [4] defines a bed mounted acoustic doppler current profiler (ADCP) as the preferred current velocity measurement device, as well its position relative to the energy extraction plane. However, since the platform swings with the flow direction, in this work an onboard Valeport Electromagentic Current Meter (ECM) close to the water surface is used. The ECM only provides a single measurement point, rather than a power-weighted aver-age of the flow at hub height as derived from a flow profile as per IEC recommendation. Though this does not comply with IEC recommendation the ECM is a more robust in-strument and was therefore selected for long term flow ve-locity measurement on the platform. The IEC method will be followed where possible to validate performance.

TABLE II
TEST INSTRUMENTATION

Parameter	Instrument	Location	Label
Power	S120 SIEMENS Inverter	Control Container	3
Torque	S120 SIEMENS Inverter	Control Container	3
Rot. Speed	S120 SIEMENS Inverter	Control Container	3
Velocity	Valeport Electromagnetic Current Meter	GP - Upstream from SIT3, 6.1m, 27cm below water	2
Reaction force at pins (Thrust)	LCM Load Pin	Lower connection point between SDM and crossdeck structure	1

Wave heights haven`t been measured throughout this study, however given the sheltered deployment location the authors do not consider an significant effect of waves on the performance results detailed in the below.

D. Downstream Wake Measurements

Measurements to characterize the turbine wake were conducted downstream of PLAT-I 4.63 using two stream-following surface drifters. Each drifter was equipped with a down-looking ADCP and a GPS tracker. Two Nortek Signature ADCPs, one 1000 kHz unit and one 500 kHz unit to avoid acoustic interference, recorded vertical profiles of along-beam velocities at 8 Hz and 4 Hz sampling frequency respectively. The GPS trackers recorded surface

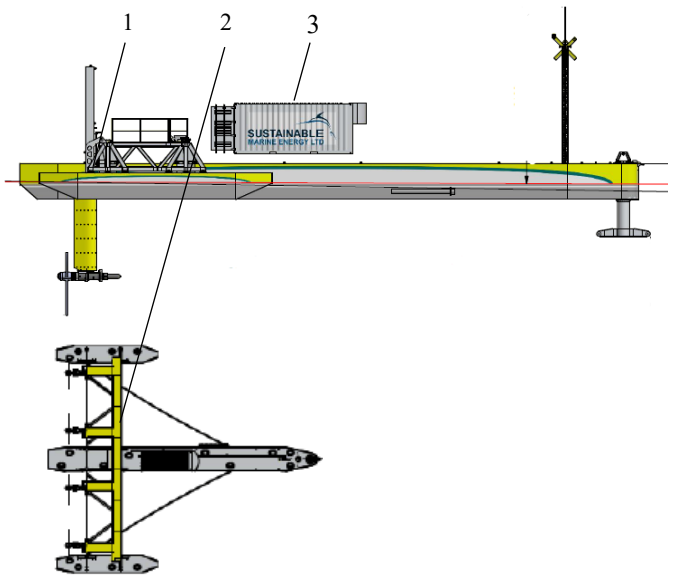

Fig. 8 PLAT-I with instrumentation locations (side and top view)

drifting velocity and drifter position along each drifter trajectory [13]. Drifters were hand-released from a small vessel just downstream of PLAT-I 4.63 at different locations parallel to the platform's cross-deck. Each drift lasted at least 90 s with distance covered ranging from 130 m to 490 m depending on tidal stage (20 d_{tip} to 78 d_{tip}, or 10 d_{equ} to 40 d_{equ}). Data were collected along 390 drifts at different phases of the tide.

IV. Data Processing

A. Post-Processing Performance

Various sampling rates were used during the data collection for different instruments and test objectives, however all data in this work was aligned to 1Hz. All data was recorded synchronously and no filtering was applied to the data sets. All post-processing was applied to the data as per IEC [4]. Further detail and equations can be found in the reference document, though key equations will be presented here. The IEC suggests using an averaging period between 2 and 10 min; the data presented here has been 2 minute averaged. In general, the following steps are performed using the bin methodology:

1. Initially, the collected data is divided into time spans of Δt = 120 s. Subsequently, the data within a distinct time span is n averaged. The arithmetic (linear) mean is used for power and thrust whereas the cubic mean ("power weighting") is applied for the inflow speed U_0:

$$\overline{U}_{0,n} = \left[\frac{1}{N_t} \sum_{j=1}^{N_t} {U_{0,j}}^3 \right]^{1/3} \quad (1)$$

$$\overline{P}_{el,n} = \frac{1}{N_t} \sum_{j=1}^{N_t} P_{el,j} \quad (2)$$

$$\overline{T}_n = \frac{1}{N_t} \sum_{j=1}^{N_t} T_j \quad (3)$$

N_t is the number of data samples within the the *n-th* time span (j = 1,…,N_t)

2. Each data set of a time span n, here $\overline{U}_{0,n}$, $\overline{P}_{el,n}$ and $\overline{T}_n$, is then assigned to the corresponding flow velocity bin i of a ΔU_0 = 0.1 m/s width.
3. Finally, the arithmetic mean of the values sorted into the *i-th* velocity bin is calculated for inflow speed, power and thrust:

$$\overline{U}_{0,i} = \frac{1}{N_i} \sum_{n=1}^{N_i} \overline{U}_{0,i,n} \quad (4)$$

$$\overline{P}_{el,i} = \frac{1}{N_i} \sum_{n=1}^{N_i} \overline{P}_{el,i,n} \quad (5)$$

$$\overline{T}_i = \frac{1}{N_i} \sum_{n=1}^{N_i} \overline{T}_{i,n} \quad (6)$$

N_i is the number of samples sorted into the *i-th* bin. The uncertainties are determined following the DIN 1319-3 [14].

B. Post-Processing Wake

Data collected by the drifting ADCPs were quality controlled to remove values with low amplitudes and correlations following the manufacturer's recommendation. The velocities were corrected for buoy motion using accelerometer data from the Signatures' integrated Attitude Heading Reference System (AHRS). The cleaned and motion-corrected along-beam velocities were then converted to Earth coordinates velocities and combined with the GPS measured drift velocities to obtain vertical profiles of Eulerian velocities along the drift trajectory. Additional details of data processing can be found in [15]. The processed data set consists of multiple vertical profiles of Eulerian velocities, each collected at a specific tidal phase (time) and location (recorded by the GPS tracker).

A local coordinate system centred at PLAT-I 4.63's nominal location and aligned with the principal direction of the flow at this location (-18.8° from true north, flood positive

northward) is defined for data organization purposes. Collected velocity profiles are first organized by tidal phase (ebb and flood) and by inflow velocity. Data corresponding to each tidal phase are then allocated to 5 x 5 m² horizontal grid cells within the local coordinate system using their GPS location. Data within each grid-cell are used to obtain ensembled-averaged vertical profiles of Eulerian velocities. The final products are maps of Eulerian velocities downstream of PLAT-I 4.63 for several stages of the tide. Data collected when blades were "fouled" and when blades were "clean" were processed separately.

V. Performance Prediction using a BEM model

An enhanced in-house BEM method for the prediction of the performance of a given turbine is used in this study. A detailed description of the model as well as a validation based on model scale and full-scale test data is given in [17]. In spanwise direction the turbine blade is segmented into a number of blade elements (BE). For every BE, the local power and thrust coefficients are derived based on momentum conservation ($C_{P,M}$ and $C_{T,M}$) and the dynamic forces on a quasi 2D hydrofoil ($C_{P,DF}$ and $C_{T,DF}$). Equating $C_{P,M} = C_{P,DF}$ and $C_{T,M} = C_{T,DF}$ yields two nonlinear equations for the unknown local axial and tangential velocity components and eventually the BEs' C_P and C_T. The overall turbine performance at a specific tip speed ratio then results from a summation over all BEs.

The hydrodynamic forces (lift and drag) for all BEs are needed to determine $C_{P,DF}$ and $C_{T,DF}$. Since lift and drag of the hydrofoil sections are functions of the Reynolds number Re and angle of attack α, they are calculated in advance and stored in a database. These polar data are obtained utilizing the public domain code XFoil [16].

Simplifying assumptions, such as a flow field that is purely 2D, are limiting the precision of the basic BEM theory. In order to increase the accuracy of the method, various sub-models are applied [18], [19], [20] and [21].

In order to evalute the effect of fouling on the lift and drag forces of the respective hydrofoils used, a parametric study is carried out. Therefore, a wide range of different percent adjustments are applied to the original polar data and the corresponding turbine performance is predicted using the in-house BEM model. As suggested in [6] both an increased drag as well as a decreased lift is investigated. A suitable combination of lift and drag changes are found for each blade condition in order to match the model performance prediction with the experimental results. The same changes are applied to all hydrofoils used within the blade design. The changes are applied to a base case polar set derived from XFoil

VI. Results

A. *Prediction of Fouling using BEM*

Normalized drag and lift coefficients against the angle of attack are shown in Fig. 9 and Fig. 10 for a hydrofoil located at 75% of the span. The drag coefficient is increased by 350% for "clean PS" and by 700% for "fouled" compared to the "clean" base case, Fig. 9. The lift coefficient, however, was reduced by 20% for the "clean PS" and by 40% for the "fouled" condition, based on $\alpha = 5$ deg, Fig. 10. These changes are significantly higher for drag when compared to wind tunnel findings as reported in [6], where the drag coefficient was only increased by 159%, whereas changes in lift are in the same order of magnitude. This is also reflected in the relative roughness, which is an order of magnitude different when comparing the wind tunnel testing in [6] ($k/c = 0.002$), with the estimate for the "fouled" full-scale rotor ($k/c \approx 0.006$-0.03).

The modified polar data as described above is used within the in-house BEM model to predict non-dimensional power and thrust characteristics as function of the tip speed ratio for the three blade conditions: "clean", "cleaned PS" and "fouled". Fig. 11 shows the effect of fouling on the power coefficient as predicted by the BEM model. It is clear, that the performance of an instream turbine is very sensitive to fouling as the maximum power coefficient drops by 49%. Furthermore, the optimum operating range is significantly narrowed and the maximum power coefficient is shifted towards lower tip speed ratios.

Fig. 12 compares the thrust characteristics for the different fouling conditions. At the operating tip speed ratio, the thrust coefficient is reduced by 22%.

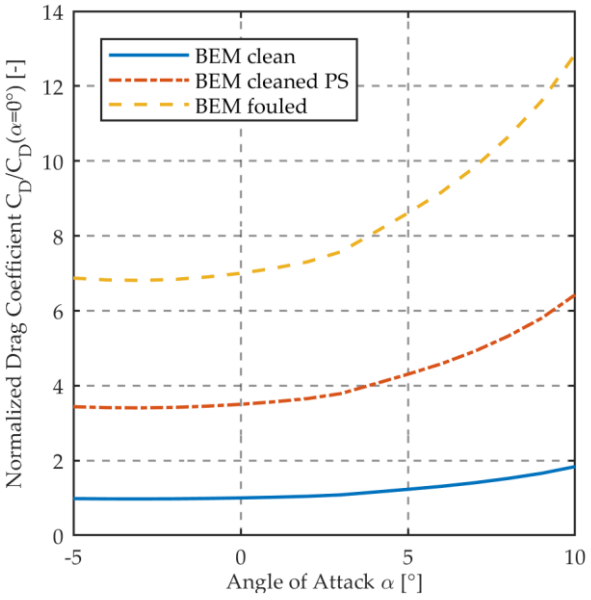

Fig. 9 Variation of the hydrofoil condition (clean, cleaned PS, fouled) and its effect on the normalized drag coefficient as function of the angle of attack

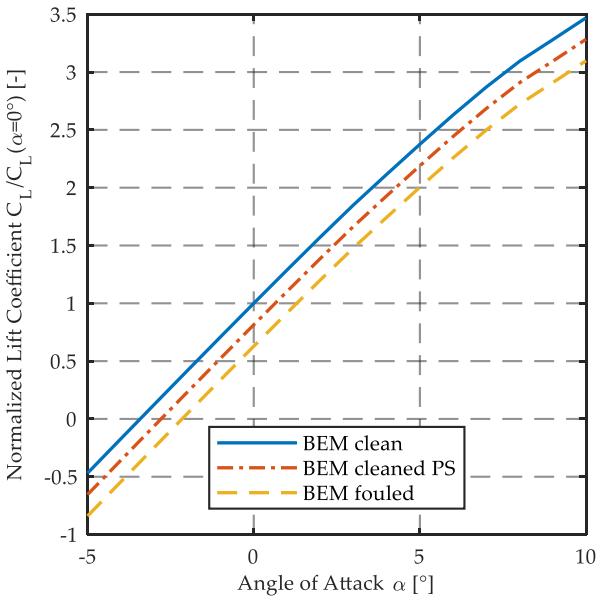

Fig. 10 Variation of the hydrofoil condition (clean, cleaned PS, fouled) and its effect on the normalized lift as function of the angle of attack

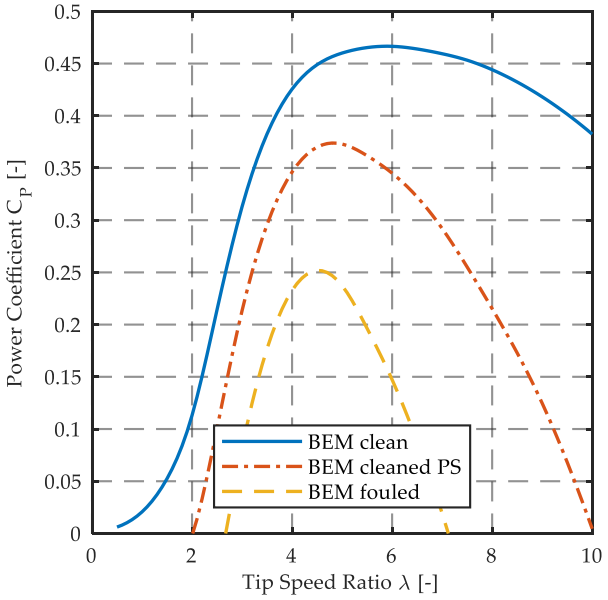

Fig. 11 Power coefficient as function of the tip speed ratio (BEM prediction of the different blade conditions)

B. *Effect of Fouling on Turbine Performance in the Field*

The power curves, obtained following the IEC procedure, are compared to the BEM prediction for the three different fouling scenarios in Fig. 13. The agreement between prediction and "clean" experimental data is highly satisfactory. Since the lift and drag properties had been selected in order for the BEM prediction to match the "cleaned PS" and "fouled" experimental results, the good agreement with the experimental data is rather expected. A performance reduction of 43% can be reported between the "clean" and "fouled" condition for inflow speeds greater then 1.6 m/s.

The thrust curves based on the load pin measurements at the SDMs are presented in Fig. 14. Above 1.6 m/s inflow speed the operational thrust is reduced by approx. 25% due to fouling.

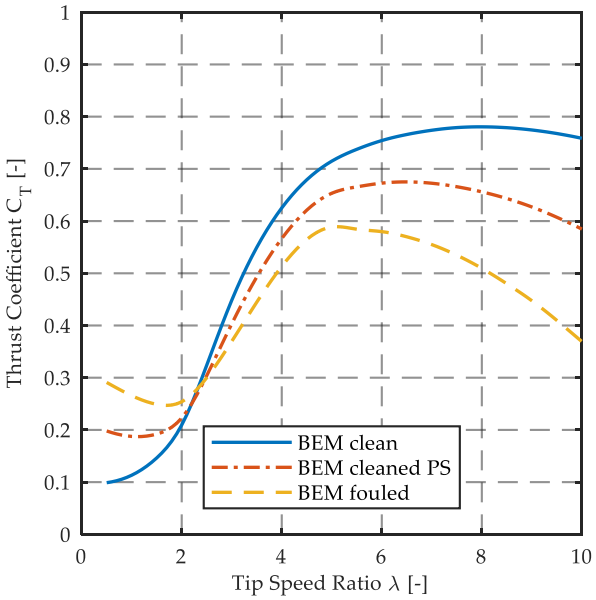

Fig. 12 Thrust coefficient as function of the tip speed ratio (BEM prediction of the different blade conditions)

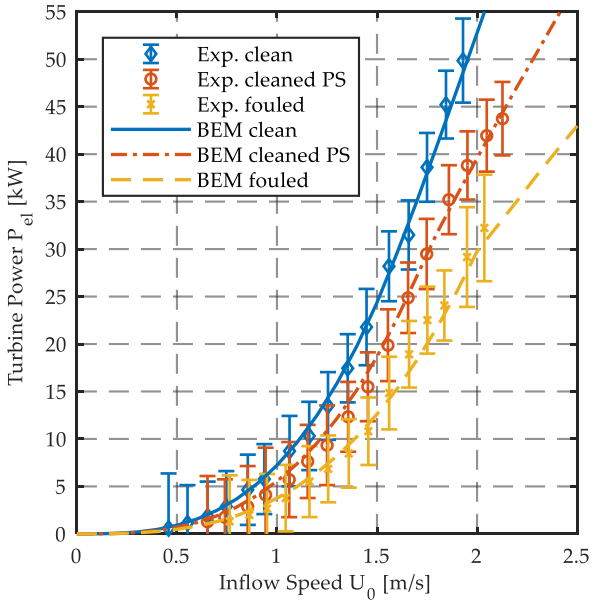

Fig. 13 Effect of fouling on the measured and BEM predicted turbine power as function of the inflow velocity

C. *Effect of Fouling on Turbine Wake*

Fig. 15 shows ensemble-averaged vertical profiles of along-channel velocity for both "clean" and "fouled" blade conditions at 5 d_{equ} (~63 m) downstream of the rotor plane. A region of reduced velocities (the wake) is observed at depths spanned by the turbine rotors. The velocity deficit

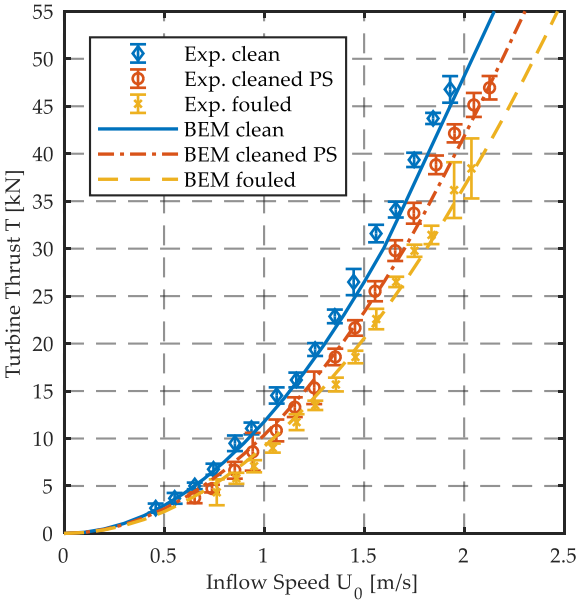

Fig. 14 Effect of fouling on the measured and BEM predicted turbine thrust as function of the inflow velocity

in the wake of "fouled" rotors is less than "cleaned" turbines case, with a 0.3 m/s additional velocity decrease when turbines are fouled when the inflow velocity is about 2 m/s. This result is consistent with Fig. 14 and Fig. 15 as "fouled" rotors extract less energy from the flow hence a weaker wake would be expected.

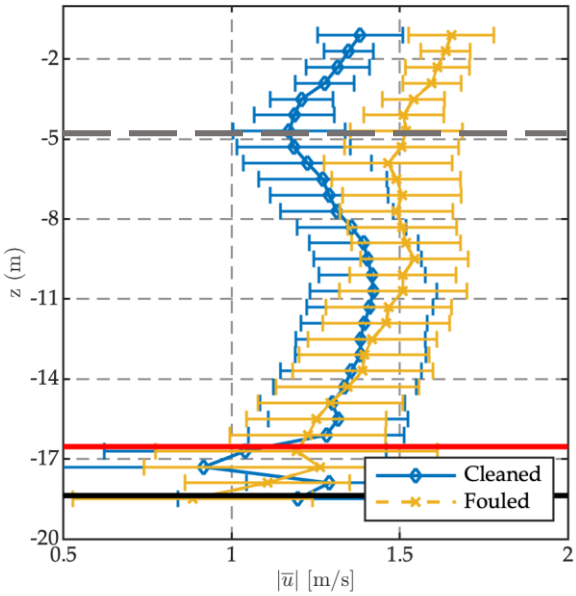

Fig. 15 Ensemble-averaged profiles of along-channel velocity for "clean" and "fouled" conditions during ebb tide at 2 m/s inflow conditions, five effective diameters downstream of the turbine. Error bars denote cross-wake variability (1 standard deviation). Grey dashed line denotes turbine hub-depth. Horizontal black line is the bottom. The horizontal red line indicates the depth at which side-lobe contamination from the bottom return begins to contaminate the velocities.

VII. Conclusion

The objective of the study was to present the effect of fouling on the full-scale in field performance characteristic of instream turbines. Three different fouling scenarios are considered: "clean", clean PS" and "fouled". The turbine was deployed from the surface floating platform PLAT-I by Sustainable Marine Energy and tested at Grand Passage, Nova Scotia. Post processing according to IEC 62600-200 has been used to evaluate the turbine performance. Measurements to characterize the turbine's wake were conducted downstream of PLAT-I 4.63 using stream-following surface drifters. A parametric study using an in-house BEM model was used to identify the change in terms of lift and drag of the respective hydrofoils. Non-dimensional as well as dimensional turbine characteristics are predicted and compared with the measured data.

The comparison of the results shows that fouling imposes a significant risk to the performance of instream turbines. A power drop of up to 47% and a thrust reduction of 28% was recognized during full scale testing for the "fouled" condition. This reflects an increase of the hydrofoil's drag coefficient by 700% and a reduction of its lift coefficients by 40%. The reduced performance is also visible in a weaker wake as the rotors extract less energy from the flow.

The presented results represent important steps towards the understanding on how fouling impacts the performance of full-scale instream turbines. The results, show the benefit of easy access to the turbines for regular inspections (including the cleaning of the rotors) to ensure high efficiency of rotors deployed on PLAT-I throughout their lifetime.

Acknowledgement

This work been funded by the Federal Ministry for Economic Affairs and Energy of Germany (BMWi) in the project OsT (FKZ 03EE4001A). The ADCP-related work was funded by the MITACS Accelerate postdoctoral fellowship programme, Luna Sea Solutions Inc., the Nova Scotia Offshore Energy Research Association (OERA), the Canada Foundation for Innovation (CFI), and the Natural Resources Canada Clean Growth Program.

References

[1] J. McNaughton, S. Harper, R. Sinclair, and B. Sellar, "Measuring and modelling the power curve of a Commercial-Scale tidal turbine", In Proc. of 11th EWTEC, Nantes, France, 6-11 Sept 2015.

[2] P. Jeffcoate, R. Starzmann, B. Elsaesser, S. Scholl and S. Bischof, "Field Measurements of a Full Scale Tidal Turbine", International Journal of Marine Energy, Volume 12, pages 3-20, 2015.

[3] R. Starzmann, I. Goebel, P. Jeffcoate: Field Performance Testing of a Floating Tidal Energy Platform - Part 1: Power Performance, In Proc. 4th Asian Wave and Tidal Energy Conference, Taipee, 2018.

[4] Marine energy – Wave, tidal and other water current converters – Part 200: Electricity producing tidal energy converters – Power performance assessment, IEC/TS 62600-200, 2014.

[5] C.C. Stringer and B.L. Polagye, "Implications of biofouling on cross-flow turbine performance", SN Appl. Sci. 2, 464, 2020.

[6] J. M. Walker, K. A. Flack, E. E. Lust, M. P. Schultz, L. Luznik, "Experimental and numerical studies of blade roughness and fouling on marine current turbine performance", Renewable Energy, Volume 66, pp. 257-267, 2014.

[7] S. Song, Y. K. Demirel, M. Atlar, W. Shi,"Prediction of the fouling penalty on the tidal turbine performance and development of its mitigation measures",Applied Energy,Volume 276, 2020.

[8] R. Starzmann, N. Kaufmann, P. Jeffcoate: Full and Model Scale Testing of Two Different Rotor Diameters for Instream Power Generation; In Proc. 13th European Wave and Tidal Energy Conference, Naples, Italy, September 2019.

[9] J. McMillan, A. Hay, R. Karsten, G. Trowse, D. Schillinger and M. O-Flaherty-Sproul, "Comprehensive Tidal Energy Resource Assessment in the lower Bay of Fundy, Canada", In Proc. of 10th EWTEC, Aalborg, Denmark, 2-5 Sept 2013.

[10] R. Karsten and M. O'Flaherty-Sproul, "Numerical modelling of Digby Neck tidal currents," OERA, Tech. Rep., March 2013.

[11] A. Hay, R. Karsten, G. Trowse, D. Morin, T. Webster, J. McMillan, M. O-Flatherty-Sproul, D. Schillinger, R. Cheel, E. Marshall and N. Crowell, "Southwest Nova Scotia Tidal Resource Assessment", OERA Technical . Report, June 2013.

[12] J. McMillan and A. Hay, "Spectral and structure function estimates of turbulence dissipation rates in a high-flow tidal channel using broadband ADCPs", J. Atmos. Oceanic Technol., 34, 5–20 doi:10.1175/JTECH-D-16-0131.1.

[13] M. Guerra and J. Thomson, "Wake measurements from a hydrokinetic river turbine." Renewable Energy 139 (2019): 483-495.

[14] DIN 1319-3, Grundlagen der Messtechnik Teil 3: Auswertung von Messungen einer einzelnen Messgröße, Messunsicherheit, Deutsches Institut für Normung; Deutsches Institut für Normung: Beuth. Berlin

[15] M. Guerra, A. Hay, R. Karsten, R. Cheel and G. Trowse, "Turbulent flow mapping in a high-flow tidal channel using mobile acoustic Doppler current profilers", In revision at Renewable Energy 2021.

[16] M. Drela, XFoil - Subsonic Airfoil Development System, 2013.

[17] N. Kaufmann, "Small Horizontal Axis Free-Flow Turbines for Tidal Currents" PhD diss., University of Siegen, December 2018.

[18] M. L. Buhl, "New Empirical Relationship between Thrust Coefficient and Induction Factor for the Turbulent Windmill State," Technical Report: NREL/TP-500-36834, National Renewable Energy Laboratory, Golden, CO, 2005.

[19] H. Glauert, "Airplane Propellers," in Aerodynamic Theory: A General Review of Progress Under a Grant of the Guggenheim Fund for the Promotion of Aeronautics, W. F. Durand, Ed., Berlin, Heidelberg: Springer Berlin Heidelberg, 1935, pp. 169–360

[20] W. Z. Shen, R. Mikkelsen, J. N. Sørensen, and C. Bak, "Tip loss corrections for wind turbine computations," Wind Energ., vol. 8, no. 4, pp. 457–475, 2005.

[21] L. A. Viterna and R. D. Corrigan, "Fixed Pitch Rotor Performance of Large Horizontal Axis Wind Turbines," in DOE/NASA Workshop on Large Horizontal Axis Wind Turbines, Cleveland, 1981.